Article

Theoretical Study of the Amazing Firefly Bioluminescence: The Formation and Structures of the Light Emitters

Galina Orlova, John D. Goddard, and Lioubov Yu. Brovko

J. Am. Chem. Soc., **2003**, 125 (23), 6962-6971• DOI: 10.1021/ja021255a • Publication Date (Web): 17 May 2003

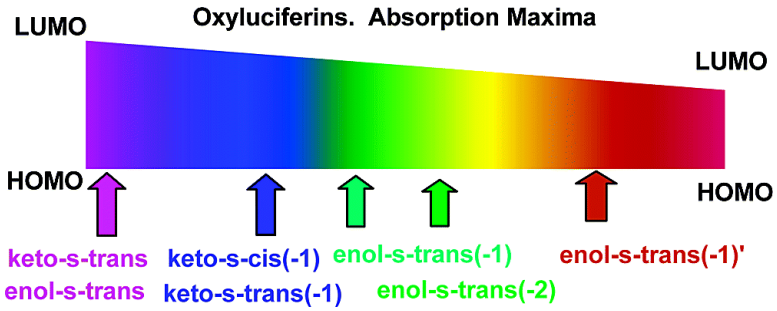

More About This Article

Additional resources and features associated with this article are available within the HTML version:

- Supporting Information
- Links to the 11 articles that cite this article, as of the time of this article download
- Access to high resolution figures
- Links to articles and content related to this article
- Copyright permission to reproduce figures and/or text from this article

View the Full Text HTML

J|A|C|S
ARTICLES
Published on Web 05/17/2003

Theoretical Study of the Amazing Firefly Bioluminescence: The Formation and Structures of the Light Emitters

Galina Orlova,[†] John D. Goddard,*[,†] and Lioubov Yu. Brovko[‡]

Contribution from the Department of Chemistry and Biochemistry, Department of Food Science, University of Guelph, Guelph, Ontario, Canada, N1G 2W1

Received October 7, 2002; E-mail: jgoddard@uoguelph.ca

Abstract: Reaction mechanisms for the formation of the keto-form of oxyluciferin ($OxyLH_2$) from the luciferin of fireflies via a dioxetanone intermediate are predicted using the B3LYP/6-31G* theoretical method. The ring opening of a model dioxetanone and the decarboxylation proceed in one step via a singlet diradical transition structure with an activation barrier of 18.1 and an exothermicity of 90.8 kcal/mol. The $S_0 \rightarrow S_1$ vertical excitation energies predicted with time dependent density functional theory, TDDFT B3LYP/6-31+G*, for the anionic and neutral forms of $OxyLH_2$ are in the range of 60 to 80 kcal/mol. These energetic results support the generally accepted theory of chemically initiated electron exchange luminescence (CIEEL). The chemical origin of the multicolor bioluminescence from $OxyLH_2$ is examined theoretically using the TDDFT B3LYP/6-31+G*, ZINDO//B3LYP/6-31+G*, and CIS/6-31G* methods. A change in color of the light emission upon rotation of the two rings in the S_1 excited state of $OxyLH_2$ is unlikely because both possible emitters, the planar keto- and enol-forms, are minima on the S_1 potential energy surface. The participation of the enol-forms of $OxyLH_2$ in bioluminescence is plausible but not required to explain the multicolor emission. According to predictions at the TDDFT B3LYP level, the color of the bioluminescence depends on the polarization of the $OxyLH_2$ in the microenvironment of the enzyme-$OxyLH_2$ complex.

Introduction

Bioluminescence, the beautiful natural phenomenon of light emission from living organisms, has attracted the attention of scientists for ages. Recently, bioluminescence has found wide and rapidly growing applications in environmental control, in biotechnology, and in molecular biology.[1] Bioluminescent techniques for the analysis of bacterial contamination are currently the fastest assays available.[2] An additional beneficial feature which distinguishes bioluminescent reactions from their chemiluminescent analogues are very high quantum efficiencies (ca. 90% for the luciferases from fireflies[3,4]). In recent years, bioluminescence from luciferase has become an extremely important tool in the study of gene expression and gene regulation.[5] A detailed knowledge of the chemical origin of the variation of the color of the bioluminescence will provide opportunities for the directed syntheses of recombinant luciferases selected for the color of light emitted. These luciferases designed for specific luminescent wavelengths could be used in the simultaneous real-time monitoring of several different gene regulation and expression events both in vitro and in vivo.

It has been established[3,4,6−9] that in all bioluminescent insects light arises from the oxidation of a substrate (a luciferin, LH_2) by an enzyme (a luciferase) that in turn results in the formation of a product (an oxyluciferin, $OxyLH_2$) in an electronically excited state. As this excited state decays to the ground state, a photon of light is emitted.[6] Firefly luciferase first catalyzes the condensation of LH_2, a derivative of benzothiazolyl-thiazole, (S)-2-(6-hydroxy-2-benzothiazolyl)-2-thiazoline-4-carboxylic acid, (Scheme 1), with adenosine-5′-triphosphate (ATP) in the presence of Mg^{2+}. It is generally accepted that the phenolic OH group of LH_2 is deprotonated and the anionic form, $LH_2(-1)$, participates in the reaction. The system undergoes one more deprotonation at C4 the acidity of which is increased due to a presence of the ATP. The product interacts with molecular oxygen with the formation of a highly energetic dioxetanone intermediate, i.e., in this step luciferase acts as an oxygenase. The strongly exothermic decarboxylation of dioxetanone leads to the keto-form of $OxyLH_2$, 2-(6′-hydroxybenzothiazol-2-yl)-4-hydroxythiazole, in an excited singlet state, S_1, which decays to the ground state with the emission of visible light. The AMP, pyrophosphate, and CO_2 are released. The deprotonation of C4 was suggested to be the rate-limiting step of the oxygenase reaction.[4b]

The reaction pathway in Scheme 1, with a dioxetanone intermediate as the key structure, reflects the generally accepted

[†] Department of Chemistry and Biochemistry.
[‡] Department of Food Science.

(1) Kricka, L. J. *Methods Enzymol.* **2000**, *305*, 333.
(2) Griffiths, M. W. *Food Technol.* **1996**, *50*, 62.
(3) McCapra, F. M.; Perring, K. D. In *Chemi- and Bioluminescence*; Burr, J. R., Ed.; New York: Dekker: 1985; p 359.
(4) (a) McElroy, W. D.; DeLuca, M. In *Chemi- and Bioluminescence*; Burr, J. R., Ed; New York: Dekker: 1985; p 387. (b) DeLuca, M.; McElroy, W. D. *Biochemistry* **1974**, *13*, 921.
(5) Roelant, C. H.; Burns, D. A.; Scheirer, W. *Biotechniques* **1996**, *20*, 914.
(6) Wilson, T.; Hastings, W. J. *Annu. Rev. Cell Dev. Biol.* **1999**, *14*, 197.
(7) (a) McCapra, F. *J. Chem. Soc. Chem. Commun*. **1977**, 946. (b) Koo, J.-Y.; Schmidt, S. P.; Schuster, G. B. *Proc. Natl. Acad. Sci. U.S.A.* **1978**, *75*, 30. (c) Schuster, G. B. *Acc. Chem. Res.* **1979**, *12*, 366.
(8) Alvarez, F. J.; Parekh, N. J.; Matuszewski, B.; Givens R. S.; Higuchi, T.; Schowen R. L. *J. Am. Chem. Soc.* **1986**, *108*, 6435.

10.1021/ja021255a CCC: $25.00

Scheme 1

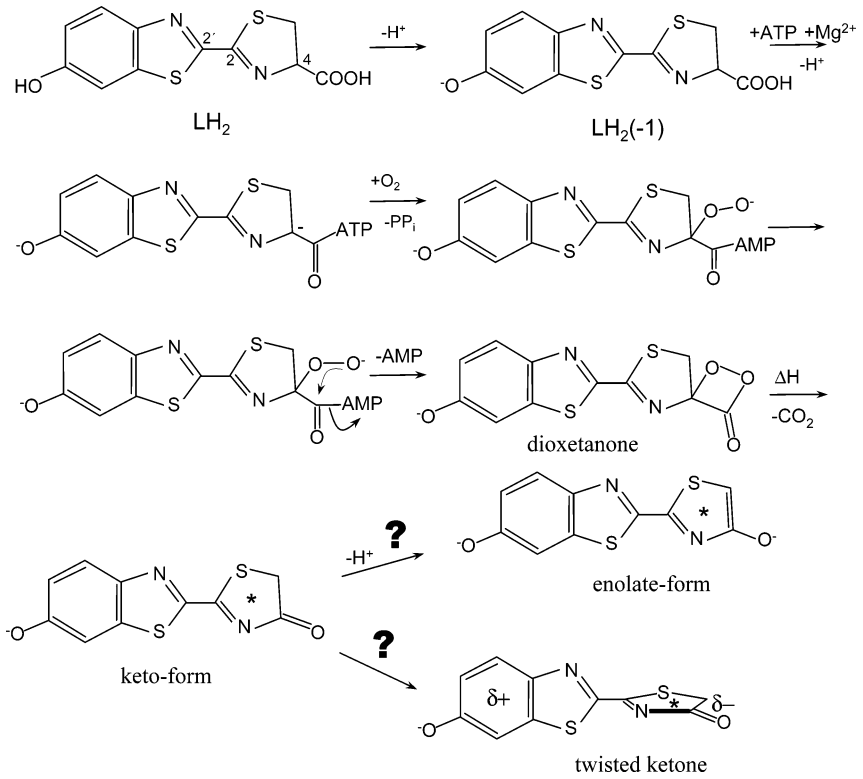

theory of Chemically Initiated Electron Exchange Luminescence (CIEEL) that was proposed by McCapra[7a] and by Schuster and co-workers.[7b,c] Several previously described bright chemiluminescent systems were interpreted by this model.[8] Despite the fact that the reaction mechanism has been intensively investigated for over 30 years, the CIEEL and the structure of the emitter are not supported by direct experimental evidence. The involvement of the dioxetanone in bioluminescence was indicated only as a plausible route to the efficient formation of an excited product.[9]

An even more intriguing problem is the chemical origin of multicolor bioluminescence. The reaction route and the substrate-product structures have been shown to be the same for all bioluminescent insects (click beetles, railroad worms, and fireflies),[10] however their emissions span a wide range of wavelengths from green (545 nm) to red (620 nm).[11−13] To explain the variation in the color of the bioluminescence, three major hypotheses were proposed. One possible mechanism involves deprotonation of the keto-form which emits red light and formation of the enolate form which was postulated to emit yellow-green light.[14] The resulting color would depend on the keto−enol equilibrium. However, recent experiments by Branchini et al.[15] demonstrated that multicolor luminescence also can be obtained from 5,5-dimethyloxyluciferin which is constrained to exist only in the keto-form. An alternative scheme was suggested by McCapra et al.[16] on the basis of theoretical predictions at the semiempirical AM1 level. According to their results,[16] the keto-form in the excited singlet state has a twisted structure rather than a planar one. The planar species is a saddle point on the S_1 potential energy surface. The color of the light emission could change upon rotation of the thiazolinone fragment about the C2−C2′ single bond. A third hypothesis assumes that the color of bioluminescence depends on the polarization of the $OxyLH_2$ in the microenvironment of the enzyme-$OxyLH_2$ complex.[17] Experiments show that the color of the light emission from $OxyLH_2$ depends on the pH of the media[17] and can be varied by modifying certain residues in the luciferase.[17]

The relationship between the wide range of bioluminescent colors and the structure of the light emitter or emitters and the mechanism of the formation of $OxyLH_2$ remain challenging problems. Experimental studies of the light emitters are hindered due to the extreme instability of $OxyLH_2$. Theoretical studies of bioluminescent phenomena are restricted to a few semiempirical models.[16,18]

In this article, hybrid density functional theory (DFT) is employed to examine the CIEEL model. The time-dependent hybrid DFT (TDDFT), configuration interaction with single

(9) McCapra, F. In *Bioluminescence and Chemiluminescence. Molecular Reporting with Photons*; Hastings, J. W.; Kricka, L. J.; Stanley, P. E., Eds. Chichester; John Wiley & Sons. 1997; p 15.
(10) Wood, K. V. *Photochem. Photobiol*. **1995**, *62*, 662.
(11) Wood, K. V.; Lam, Y. A.; Seliger, H. H.; McElroy, W. D. *Science*, **1989**, *244*, 700.
(12) Ugarova, N. N. *J. Biolum. Chemilum*. **1989**, *4*, 406.
(13) (a) Viviani, V. R.; Bechara, E. J. H. *Photochem. Photobiol*. **1995**, *62*, 490. (b) Viviani, V. R. *Cell. Mol. Life Sci.* **2002**, *59*, 1833.
(14) White, E. H.; Rapaport, E.; Seliger, H. H., McElroy, W. D. *Bioorg. Chem*. **1971**, *1*, 92.
(15) Branchini, B. R.; Murtiashaw, M. H.; Magyar, R. A.; Portier, N. C.; Ruggiero, M. C.; Stroh, J. G. *J. Am. Chem. Soc*. **2002**, *124*, 2112.
(16) McCapra, F.; Gilfoyle, D. J.; Young, D. W.; Church, N. J.; Spencer, P. In *Bioluminescence and Chemiluminescence. Fundamentals and Applied Aspects*; Campbell, A. K., Kricka, L. J., Stanley, P. E., Eds.; Chichester, John Willey & Sons: New York, 1994; p 387.
(17) (a) DeLuca M. *Biochemistry*, **1969**, *8*, 160. (b) Ugarova, N. N.; Brovko, L. Y. *Russian Chemical Bulletin*, **2001**, *50*, 1752. (c) Ugarova, N. N.; Brovko, L. Y. Luminescence, **2002**, *17*, 321**.** (d) Gandelman, O. A.; Brovko, L. Yu.; Ugarova, N. N.; Chikishev, A. Yu.; Shkurimov, A. P. *J. Photochem. Photobiol. B: Biol*. **1993**, *19*, 187.
(18) (a) Wada, N.; Honda, M.; Yoshihara, T.; Suzuki, H. *J. Phys. Soc., Jpn*. **1980**, *49*, 1519. (b) Wada, N.; Honda, M.; Suzuki, H. *J. Phys. Soc., Jpn*. **1985**, *54*, 4851.

Scheme 2

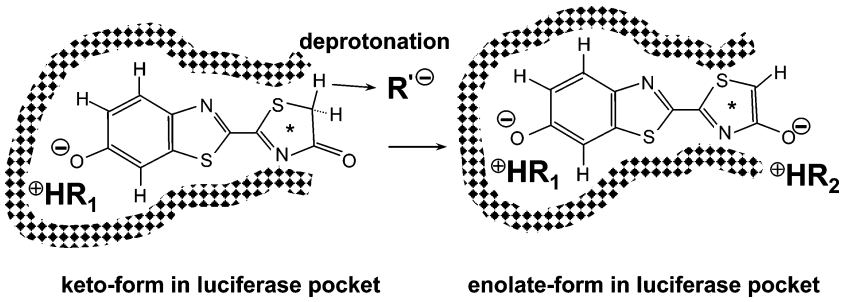

keto-form in luciferase pocket enolate-form in luciferase pocket

excitations (CIS), and the semiempirical ZINDO methods are used to study aspects of the three hypotheses regarding the $OxyLH_2$-based light emitters from fireflies. At the ab initio level of theory, the size of the enzyme-LH_2 complex makes computations prohibitive. Thus, a model for the "polarization in the microenvironment" of keto-and enol- $OxyLH_2$ was designed as follows: The structure of the luciferase-LH_2 complex has been modeled previously by Branchini et al.[19a] and by Sandalova and Ugarova [19b] using molecular mechanics (MM) combined with the X-ray data available for a luciferase enzyme without the bound substrate luciferin, ATP, or magnesium ion. According to these modeling studies,[19] LH_2 is completely buried in the protein and resides in a "pocket" which contains mostly glycine residues [19b]. The acidic group of the thiazole fragment resides at the opening of this pocket (Sketched in Scheme 2.) with the imidazole group of the histidine (His) residue in close proximity to this acidic group. The benzothiazolyl fragment lies buried deeply in the pocket of the luciferase where its phenolic OH group interacts with an amino acid residue, probably arginine, in the bottom of the pocket. (R_1 is used in Scheme 2 to represent an amino acid as one other than arginine might be involved.) After the reaction of the LH_2 with molecular oxygen, keto-$OxyLH_2$ is formed. The thiazolinone fragment of $OxyLH_2$ which resides at the opening of the pocket may interact with the environment (residues, solvents) and deprotonate to yield an enolate of oxyluciferin (Scheme 2). This enolate may coordinate with an amino acid residue or with solvent, R_2, at the opening of the pocket. According to the model for the color of bioluminescence which emphasizes the polarization of $OxyLH_2$ in the microenvironment of the enzyme-$OxyLH_2$ complex,[17] the degree of polarization of the H−O bond in the keto-complex, R_1...H...O ($OxyLH_2$) is critical. For the enol-form, the polarizations of both H−O bonds in the complex, R_1...H...O($OxyLH_2$)O...H...R_2, affect the color of bioluminescence. A strong polarization results in an ionic complex while weaker polarization gives the H-bonded complexes (for example, for the keto-form, the ion pair $R_1H^+...^-O(OxyLH_2)$ and the hydrogen bonded system R...H−O($OxyLH_2$), respectively). The strength of the polarization of the H−O bonds and, thus, the color of bioluminescence depend on the basicity of the R_1 and R_2 amino acid residues. In our computational model, the amino acid residues, R_1 and R_2, are not included and the neutral and anionic forms of the parent LH_2 and of the keto- and enol- derivatives of $OxyLH_2$, **1**−**10**, (Chart 1) are examined. These neutral and anionic forms represent the limiting ionic (strongest polarization) and hydrogen bonded (weakest polarization) cases.

Chart 1

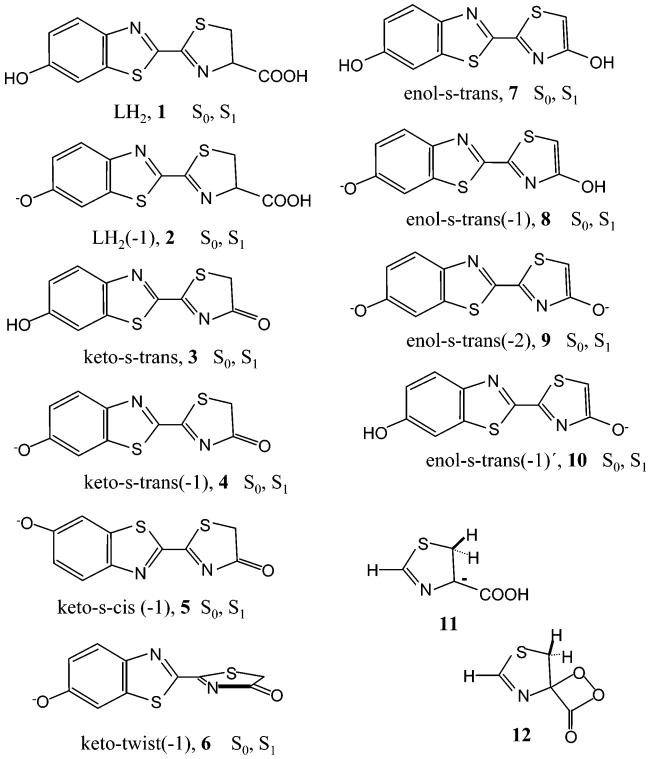

Scheme 3

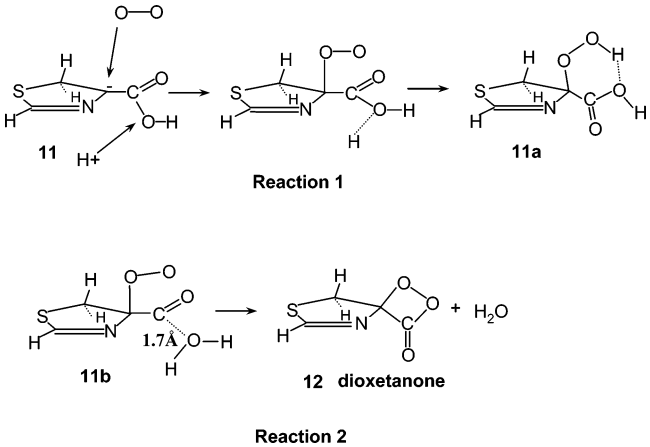

To study the formation of $OxyLH_2$ in an excited electronic state via a dioxetanone intermediate (i.e., the CIEEL model), reactions 1 and 2 (Scheme 3) between the thiazole fragment, **11**, and molecular oxygen were studied using DFT. The reaction path leads to dioxetanone, **12**, and then to the decarboxylation of this dioxetanone yielding the keto-form, thiazolinone. The

(19) (a) Branchini, B. R.; Magyar, R. A.; Murtiashaw, M. H.; Anderson, S. M.; Zimmer, M. *Biochemistry* **1998**, *37*, 15 311. (b) Sandalova, T. P.; Ugarova, N. N. *Biochemistry (Moscow)* **1999**, *64*, 962.

benzothiazolyl ring, which is present in LH_2 should not affect greatly the mechanisms of these reactions which involve the thiazole fragment and which occur at the opening of the luciferase pocket (Scheme 2).

Computational Details

Most of the theoretical predictions were made with the GAUSSIAN98 [20] program suite using predominantly hybrid density functional theory (DFT). Becke's hybrid exchange functional B3 [21] and the correlation functional of Lee, Yang, and Parr (LYP)[22] were employed. The 6-31+G*[23] split-valence basis set augmented with *d*-type polarization functions and with diffuse functions for all heavy atoms was used. For predictions of the model reactions of the thiazole fragment, the 6-31G* basis set was employed. Excited-state energy predictions were carried out using the rigorous time-dependent hybrid DFT method (TDDFT).[24,25] This relatively new computational method has been successfully employed in the prediction of the excited states of furan and pyrrole,[26a] of tetrathiafulvalene,[26b] of the caratenoids of purple bacteria,[26c] and of red fluorescent protein from coral.[26d] For additional calibration, Zerner's intermediate neglect of differential overlap (ZINDO)[27] semiempirical method was employed at the optimized B3LYP/6-31+G* geometries. Gross et al.[26d] noted that for polypeptides, ZINDO//B3LYP, in general, more closely reproduced the experimental absorption wavelengths than did B3LYP TDDFT. A number of semiempirical computations on the ground and lowest singlet excited states of oxyluciferin were performed using the AM1 model within the MOPAC2002 [28a] module of CAChe[28b] to contextualize earlier studies by McCapra et al.[16]. A computationally cost-effective excited-state method, configuration interaction with single excitations (CIS),[29] based on the Hartree−Fock method with the 6-31G* basis set was used for geometry optimization and predictions of vibrational frequencies for two likely emitters, keto-s-trans (−1) and enol-s-trans (−1), in the ground and first excited singlet electronic states. An inclusion of diffuse function is necessary for the accurate prediction of excitation energies. However, any further increase in the basis set lead to severe convergence problems at the Hartree−Fock level. The CIS/6-31G* method is expected to overestimate considerably the excitation energies but to predict plausible changes in geometrical parameters upon the $S_0 \rightarrow S_1$ excitations as well as the correct characters of critical points on the S_1 potential energy surfaces.[29a]

The singlet diradical transition structure for the ring-opening reaction of dioxetanone was located using the "guess=mix" option in GAUSSIAN98 for a formally closed shell electronic species. All relative energies reported include zero point vibrational energy corrections.

The Cartesian coordinates and total energies of the optimized structures are provided as Supporting Information.

Results

Formation of Dioxetanone. The dioxygen molecule has a triplet electronic ground state and its attachment to the closed shell LH_2 to yield a singlet complex is a spin-forbidden process. This reaction[30a] and many others between triplet dioxygen and diamagnetic organic molecules in vivo have been proposed to occur via a stepwise diradical mechanism. The reductive activation of triplet dioxygen by glucose oxidase, a potentially similar reaction in its initial steps to that of dioxygen with luciferase, was scrutinized[30b,c] recently using the B3LYP theoretical method. A detailed model was developed with the triplet dioxygen molecule coordinated between the protonated His (RH^+) and the active site of glucose oxidase (M). An electron transfers in the $RH^+...O_2...M$ complex and the $RH^+...O_2^{-\bullet}...^{+\bullet}M$ triplet diradical results. This electron-transfer proceeds without energetic barrier because the spin multiplicity (triplet) is not changed. Focusing on the oxygen in the complex, electron transfer is favored by its increased electron affinity due to the proximity of the protonated histidine residue. For the $RH^+...O_2^{-\bullet}...^{+\bullet}M$ *triplet* diradical, there is a high probability for intersystem crossing (from triplet diradical to singlet diradical). The increased spin−orbit coupling in the dioxygen species which now more closely resembles superoxide than neutral dioxygen increases the efficiency of the intersystem crossing. The interactions of the corresponding molecular orbitals of the $O_2^{-\bullet}$ and the $^{+\bullet}M$ moieties favor the crossing with the formation of the O−M bond in a singlet electronic state being energetically down hill. The $RH^+...O_2^{-\bullet}...^{+\bullet}M$ *singlet* biradical complex is produced followed by the exothermic formation of the products in a closed singlet electronic state. It has been shown that this multistep spin-flip process does not depend on the nature of M. It is important to the use of this model that a critically significant His residue resides in the proximity of the acidic group of LH_2 quite similar to the arrangement in the $HisH^+$-oxygen-glucose oxidase complex. Moreover, the photodestruction of this His residue has been shown to inactivate luciferase almost completely.[31] Thus, it is highly plausible that a similar spin-flip mechanism involving triplet and singlet biradical complexes operates in the case of oxygenation by luciferase. Because the energetically feasible spin-flip process is not the rate-limiting step, the subsequent reaction of the complex between singlet dioxygen and the thiazole fragment, **11** was studied.

Reaction pathways 1 and 2 in Scheme 3 for the formation of dioxetanone are examined at the B3LYP/6-31G* level. Reaction 1 models the attack of an oxygen molecule on the deprotonated carbon atom with the total system in a singlet state along with the simultaneous attack of a proton on the OH group to form a water molecule**.** The water is simulating the AMP leaving group

(20) Gaussian98 (Rev. A.11) Frisch, M. J.; Trucks, G. W.; Schlegel, H. B.; Scuseria, G. E.; Robb, M. A.; Cheeseman, J. R.; Zakrzewski, V. G.; Montgomery, J. A.; Stratmann, R. E.; Burant, J. C.; Dapprich, S.; Millam, J. M.; Daniels, A. D.; Kudin, K. N.; Strain, M. C.; Farkas, O.; Tomasi, J.; Barone, V.; Cossi, M.; Cammi, R.; Mennucci, B.; Pomelli, C.; Adamo, C.; Clifford, S.; Ochterski, J.; Petersson, G. A.; Ayala, P. Y.; Cui, Q.; Morokuma, K.; Salvador, P.; Dannenberg, J. J.; Malick, D. K.; Rabuck, A. D.; Raghavachari, K.; Foresman, J. B.; Cioslowski, J.; Ortiz, J. V.; Baboul, A. G.; Stefanov, B. B.; Liu, G.; Liashenko, A.; Piskorz, P.; Komaromi, I.; Gomperts, R.; Martin, R. L.; Fox, D. J.; Keith, T.; Al-Laham, M. A.; Peng, C. Y.; Nanayakkara, A.; Challacombe, M.; Gill, P. M. W.; Johnson, B. G.; Chen, W.; Wong, M. W.; Andres, J. L.; Gonzalez, C.; Head-Gordon, M.; Replogle, E. S.; Pople, J. A.; Gaussian, Inc., Pittsburgh, PA, **2001**.
(21) Becke, A. D. *J. Chem. Phys*. **1993**, 98, 5648.
(22) Lee, C.; Yang, W.; Parr, R. G. *Phys., Rev. B*, **1988**, 37, 785.
(23) Hehre, W. J.; Ditchfield, R.; Pople, J. A. *J. Chem. Phys*. **1972**, 56, 2257.
(24) Gross, E. K. U.; Kohn, W. *Adv. Quantum Chem*. **1990**, 21, 255.
(25) Casida, M. E. In *Recent Advances in Density Functional Methods*; Chong, D. P., Ed.; World Scientific: Singapore, 1995; p 155.
(26) (a) Burcl, R.; Amos, R. D.; Handy, N. C. *Chem. Phys. Lett*. **2002**, *355*, 8. (b) Pou-Amérugo, R.; Viruela, P. M.; Viruela, R.; Rubio, M.; Ortí, E. *Chem. Phys. Lett*. **2002**, *352*, 491. (c) Hsu, C.-P.; Walla, P. J.; Head-Gordon, M.; Fleming, G. R. *J. Phys. Chem. B*. **2001**, *105*, 11 016. (d) Gross, L. A.; Baird, G. S.; Hoffman, R. C.; Baldridge, K. K.; Tsien, R. Y. *PNAS* **2000**, *97*, 11 990.
(27) (a) Zerner, M. C. In *Reviews of Computational Chemistry*; Lipkowitz, K. B., Boyd, D. B., Eds.; VCH: New York, 1991; pp 313. (b) Correa de Mello, P.; Hehenberger, M.; Zerner, M. C. *Int. J. Quantum Chem*. **1982**, *21*, 251.
(28) (a) Stewart, J. J. P. MOPAC2000, Fujitsu Limited, Tokyo, Japan 1999; (b) CAChe, Version 5.0; Cache Group, Fujitsu, Beaverton, OR 2001.
(29) (a) Foresman, J. B.; Head-Gordon, M.; Pople, J. A.; Frisch, M. J. *J. Phys. Chem*. **1992**, *96*, 135. (b) Foresman, J. B.; Head-Gordon, M.; Pople, J. A.; Frisch, M. J. *J. Phys. Chem*. **1996**, *100*, 4160.
(30) (a) McCapra, F. *Methods in Enzymology*, **2000**, *305*, 3. (b) Prabhakar, R.; Siegbahn, P. E. M.; Minaev, B. F.; Ågren, H. *J. Phys. Chem. B* **2002**, *106*, 3742. (c) Minaev, B. F. *RIKEN Rev*. **2002**, *44*, 147.
(31) Branchini, B. R.; Magyar, R. A.; Marcantonio, K. M.; Newberry, K. J.; Stroh, J. G.; Hins, L. K.; Murtiashaw, M. H. *J. Biol. Chem*. **1997**, *272*, 19 359.

involved in the biological reaction as shown in Scheme 1. With the B3LYP/6-31G* method, both of these attacks proceed without barriers. However, the four-membered ring of dioxetanone is not produced by Reaction 1 because the oxygen molecule forms only one carbon−oxygen bond. Geometry optimization leads to an intermediate complex, **11a**, where a hydrogen atom transfers from the OH_2 fragment to the O−O fragment and forms an O−H···O bridge. This complex does not proceed to the dioxetanone.

Reaction 2 models the situation where the oxygen molecule attacks **11b** after the OH group has been protonated to produce an excellent leaving group. Formation of the H_2O molecule and the C−(OH_2) bond cleavage (the C−OH_2 distance in **11b** is 1.7 Å) have occurred. Under such circumstances, the formation of the dioxetanone **12** occurs spontaneously and a water molecule leaves. These model reactions reveal that the cleavage of the C-AMP (C−OH_2 in our model) bond is a key step in the reactions shown in Scheme 1. Because AMP is known to be a good leaving group in vivo its detachment should proceed via a low barrier with the formation of the metastable dioxetanone. These results support an earlier suggestion [4b] that the abstraction of the proton from C4 is the rate-limiting step in the oxygenation of adenyl-luciferin by firefly luciferase.

Reaction Mechanism for the Ring Opening and the Decarboxylation of the Dioxetanone Intermediate. According to the CIEEL model, the dioxetanone undergoes a decarboxylation which is sufficiently exothermic to promote the $OxyLH_2$ into its S_1 excited electronic state from the ground, S_0, electronic state. To our knowledge, no experimental data or theoretical predictions on the decarboxylation of this dioxetanone have been reported. An analogue of dioxetanone, the four-membered ring, dioxetane (H_4CO_2), has been studied and its decomposition to a mixture of formaldehyde molecules, in the ground state, triplet and a small amount of excited singlet was examined both experimentally[32a−b] and theoretically.[32c−d] Theoretical studies by the Robb and Olivucci groups[32c−d] showed that the ring-opening of dioxetane proceeds via a singlet diradical transition structure, with the O−O bond broken. The reaction barrier predicted with the CASSCF/MP2 method is 16 kcal/mol (the experimental value is 22 kcal/mol).[32d] The C−C bond cleavage and detachment of formaldehyde follows from the diradical transition structure without a further barrier.

The reaction profile for the ring opening and the decarboxylation of dioxetanone, **12**, predicted with the B3LYP/6-31G* method are shown in Figure 1. The reaction proceeds over a barrier of 18.1 kcal/mol. The transition structure has well-developed singlet diradical character, with an $\langle S^2 \rangle$ value equal to 0.773 and with the O−O bond broken at a distance of 2.109 Å. The C−C bond in the four-membered ring elongates by 0.031 Å to 1.563 Å. The deviation from planarity in the O−C−C−O fragment is only 4.1°. The transition vector points directly toward the products, carbon dioxide and the thiazalinone. The distance between the thiazalinone fragment and the CO_2 fragment increases and the $\langle S^2 \rangle$ value decreases gradually on

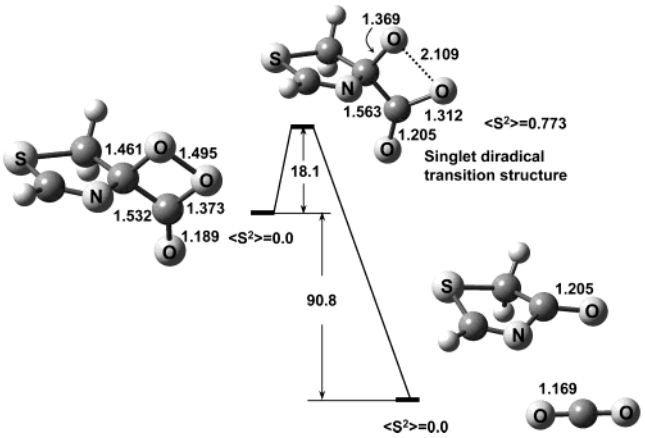

Figure 1. Potential energy profile for the ring opening and decarboxylation reaction of the dioxetanone derivative of the thiazole fragment of $OxyLH_2$ predicted with the B3LYP/6-31G* method. Relative energies (in kcal/mol) include zero-point vibrational energy corrections. Key geometrical features are reported in Å.

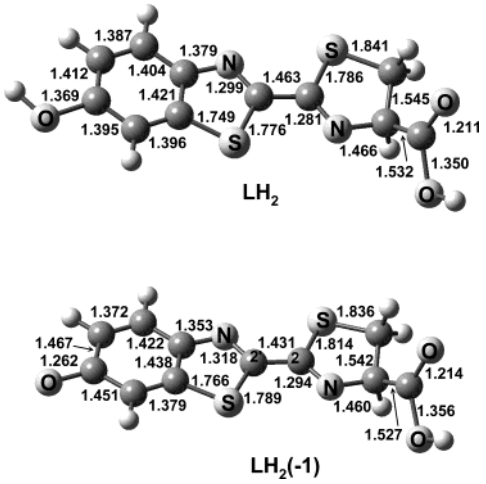

Figure 2. Selected geometrical parameters (in Å) predicted for luciferin (LH_2) and its phenolate, $LH_2(-1)$ with the B3LYP/6-31+G* method.

proceeding along the gradient line toward the products in their ground singlet electronic states. No transition structures or intermediate were found along this path, thus, the decarboxylation of the dioxetanone intermediate proceeds in one step similar to the cleavage of the simpler dioxetane. The reaction is strongly exothermic (by 90.8 kcal/mol) with the B3LYP/6-31G* method. The exothermicity should be sufficient to promote the keto-form from the ground electronic state to the lowest singlet excited state and to cause the structural rearrangements in the light emitter.

Luciferin. The parent compound of the emitters is luciferin, LH_2, which is relatively stable and fairly well-studied experimentally. According to experimental data, the absorption maximum for LH_2, λ_{max}, occurs at 330 ± 2 nm and the peak position does not depend appreciably on solvent [17c]. The ground-state geometries of LH_2 and of its phenolate form, LH_2 (−1), as predicted with B3LYP/6-31+G* are shown in Figure 2. Both LH_2 and LH_2 (−1) have nearly planar ring structures, with a very slightly pyramidal C2′ carbon atom. The rigorously planar structures for both are predicted to be first-order saddle points on the potential energy surfaces. The C2−C2′ bond distances between the benzothiazolyl and the thiazole fragments (1.463 Å for LH_2 and 1.431 Å for LH_2 (−1)) are notably shorter than

(32) (a) Adam, W. In *Chemical and Biological Generation of Excited States*; Adam, W., Cilento, G., Eds.; Academic Press: New York, 1982; p 129 (and references therein); (b) Adam, W.; Baader, W. J. *J. Am. Chem. Soc.* **1985**, *107*, 410. (c) Reguero, M.; Bernardi, F.; Bottoni, A.; Olivucci, M.; Robb, M. A. *J. Am. Chem. Soc.* **1991**, *113*, 1566. (d) Wilsey, S.; Bernardi, F.; Olivucci, M.; Robb, M. A.; Murphy, S.; Adam, W. *J. Phys. Chem. A* **1999**, *103*, 1669.

Table 1. Vertical Excitation Energies, ΔE, in eV, Excitation Wavelengths, λ, in nm, (values in parentheses are from ZINDO), Oscillator Strengths, *f*, and Corresponding Kohn−Sham (KS) Orbitals (see Figure 3) Predicted for the First Three Singlet Excited States of Luciferin (LH_2) and Deprotonated Luciferin (LH_2^{-1}) in the Gas Phase with TDDFT Using the B3LYP Functional and the 6-31+G* Basis Set

state	ΔE	λ	f	KS orbitals
LH_2/S_1	3.74	331.5 (326.0)	0.1601	0.502: HOMO-1 → LUMO 0.439: HOMO → LUMO
S_2	3.85	322.0	0.2974	0.439: HOMO-1 → LUMO −0.473: HOMO → LUMO
S_3	4.06	305.5	0.0867	0.660: HOMO-2 → LUMO
Exp.[17c]		327[a]		
LH_2^{-1}/S_1	2.61	474.5 (493)	0.3610	0.518: HOMO → LUMO
S_2	2.81	440.8	0.2268	−0.588: HOMO → LUMO+1
S_3	2.92	424.1	0.0250	−0.696: HOMO → LUMO+2
Exp.[17c]		380[b]		

[a] Aqueous solution at pH = 1. [b] Aqueous solution at pH = 10.

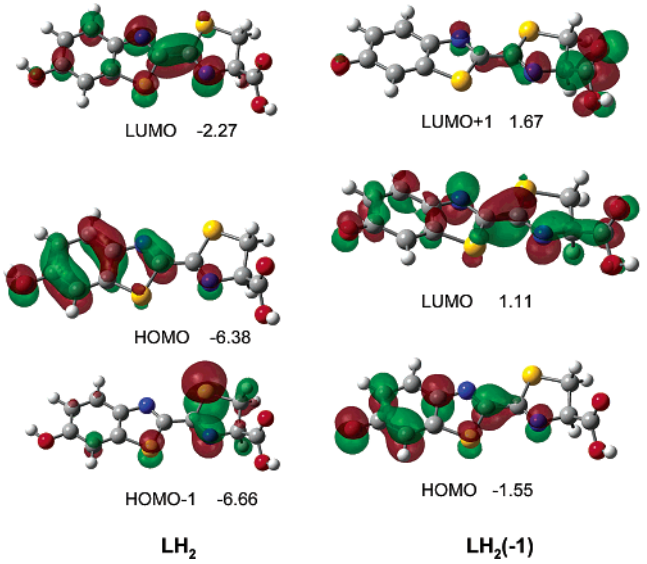

Figure 3. Kohn−Sham frontier orbitals for LH_2 and $LH_2(-1)$ predicted with the B3LYP/6-31+G* method. The Kohn−Sham orbital energies are in eV.

conventional C−C single bonds and are indicative of conjugation in the −N═C−C═N− moiety.

The TDDFT B3LYP/6-31+G* predictions of the vertical excitations for the first three excited singlet states of LH_2 and LH_2 (−1) in the gas phase are summarized in Table 1. For both the LH_2 and LH_2 (−1) species, the $S_0 \rightarrow S_1$ and $S_0 \rightarrow S_2$ transitions are allowed and have large oscillator strengths. These transitions correspond to excitations to the LUMO which is essentially a C2−C2′ π-orbital as can be seen in the plots of the Kohn−Sham (KS) frontier orbitals of LH_2 and LH_2 (−1) in Figure 3. Qualitative analysis of the KS orbitals shows that upon excitation to the S_1 state the −N═C−C═N− structure moves toward the ═N−C═C−N═ form, with an increased π−component in C2−C2′. For LH_2, the lowest two maxima of the absorption spectrum (322 nm to S_2 and 331.5 nm to S_1) predicted with TDDFT are in very good agreement with experimental data. The predicted wavelength with ZINDO (326 nm to S_1) also is in accord both with the experiment and with the TDDFT results.

The absorption spectra of LH_2 obtained experimentally [17c] in aqueous solution are shifted from 327 (pH = 1) to 380 (pH = 10) nm with the change in pH from strongly acidic to alkaline. The shift is due to the deprotonation of the OH-group in the benzothiazole fragment. For the limiting case, the LH_2 (−1) anion in the gas phase, even a greater shift to longer wavelength is expected. Indeed, for LH_2 (−1), absorption maxima at 474.5 and 493 nm are predicted with B3LYP TDDFT and with ZINDO, respectively. The reason for the considerable red shift is that deprotonation of the phenol group changes the C2−C2′ bond from single to essentially double as can be seen by examination of the KS HOMO and LUMO of LH_2 (−1) in Figure 3. The HOMO−LUMO gap and the excitation energies decrease dramatically in the anionic as compared to the neutral luciferin.

CIS Predictions on OxyLH_2. Because the S_1 states of LH_2 and LH_2 (−1) involve excitations to the LUMO which as seen in Figure 3 is a polarized π−bond between C2−C2′, rotation about this bond is unfavorable. Such a rotation in the lowest excited state of the keto-form of OxyLH_2 which has frontier orbitals similar to those in parent LH_2 was proposed as a key factor in the production of multicolor bioluminescence [16]. However, the AM1 semiempirical method which provided the earlier theoretical support for this hypothesis is now well-known[33,34] to underestimate the strength of 'conjugated single' bonds such as the C2−C2′ bond in LH_2. The rotational barriers about the C2−C2′ bond mirror the difference in the electronic structure of the −N═C−C═N- moiety predicted with semiempirical and ab initio theory. For the keto-s-trans (−1) form, the barriers to internal rotation about the C2−C2′ bond are 16.8 and 19.9 kcal/mol with HF/6-31G* and the more reliable B3LYP/6-31+G* methods versus 7.7 kcal/mol with the semiempirical AM1 model [16]. The CIS/6-31G* ab initio method was employed to examine the geometries and the character of critical points on the S_1 potential energy surfaces for the most plausible OxyLH_2 structures, keto-s-trans(−1) and enol-s-trans(−1). Selected geometries and energetics are shown in Figure 4. The enol-s-trans (−1) tautomeric species is 22.8 and 21.9 kcal/mol higher in energy than the keto-s-trans (−1) structure on the S_0 and S_1 potential energy surfaces, respectively. For both the keto- and enol-forms, the $S_0 \rightarrow S_1$ excitation affects predominantly the structure of the −N═C−C═N- unit as the bonding becomes more delocalized. Very minor structural changes are predicted for the rest of the system. This observation is consistent with an extraordinary high quantum yield of bioluminescence from the luciferases of fireflies since relatively little change in geometries is required during the $S_0 \rightarrow S_1 \rightarrow S_0$ transformations. Both the keto-s-trans(−1) and enol-s-trans(−1) planar structures correspond to minima on the S_1 potential energy surfaces, in contrast to earlier reported AM1 results [16]. For the twisted keto-anion, which was proposed earlier as a light emitter [16], the excitation to S_1 is forbidden and that to S_2 is allowed according to the CIS results. The twisted keto-anion on the potential energy surface of the S_2 electronic state is not a minimum or transition state but a third-order saddle point.

Keto-Forms of Oxyluciferin. The geometries predicted by B3LYP/6-31+G* for the three possible keto-structures, the neutral keto-s-trans molecule and the anion, keto-s-trans (−1) and its conformer, keto-s-cis (−1), are shown in Figure 5. These systems reveal the same trends as in the LH_2 and LH_2 (−1)

(33) Jensen, F. *Introduction to Computational Chemistry*; Wiley: New York, 1999; p.89.
(34) Cramer, C. J. *Essentials of Computational Chemistry. Theories and Models*; Wiley: New York, 2002; p 139.

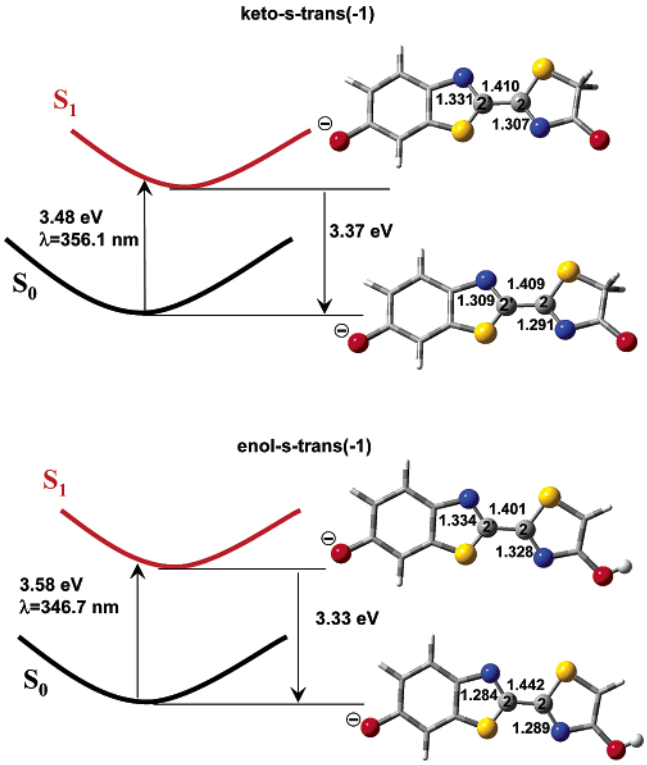

Figure 4. Keto-s-trans(−1) and enol-s-trans(−1) structures optimized in S_0 and S_1 electronic states with the CIS/6-31G* method. Selected geometrical parameters are in Å. Vertical excitation energies, the maxima of absorption, and the adiabatic energy differences between minima on the S_0 and S_1 potential energy surfaces are reported.

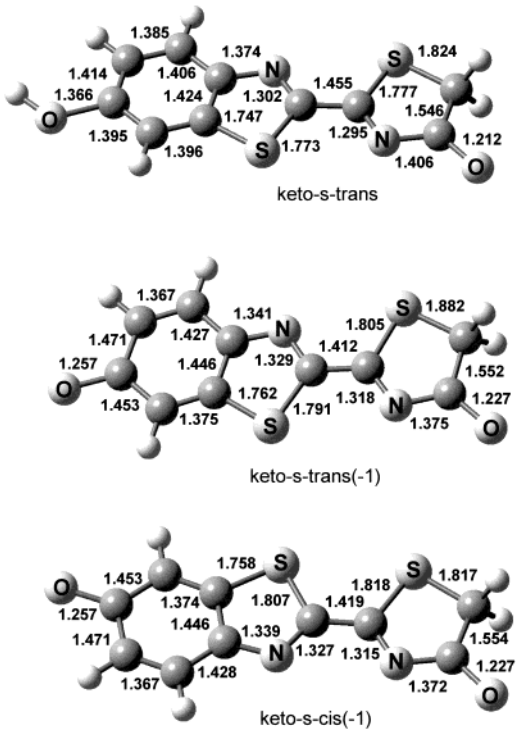

Figure 5. Selected geometrical parameters (in Å) predicted for the keto-s-trans, keto-s-trans(−1), and keto-s-cis(−1) structures of $OxyLH_2$ with the B3LYP/6-31+G* method.

pair. The rings in the keto-forms are very nearly planar, with a slightly pyramidal C2′ atom. The −N=C−C=N−C=O moiety has more localized bond lengths, i.e., slightly greater bond length

Table 2. Vertical Excitation Energies, ΔE, in eV, Excitation Wavelengths, λ, in nm (values in parentheses are from ZINDO), and Oscillator Strengths, *f*, Predicted for the First Three Singlet Excited States of Keto-*s-trans*, Keto-*s-trans*(−1), and Keto-*s-cis*(−1) Forms of Oxyluciferin in Gas Phase with TDDFT Using the B3LYP Functional and the 6-31+G* Basis Set

state	ΔE	λ	*f*
		keto-*s-trans*	
S_1	3.32	373.6 (394.4)	0.2927
S_2	3.42	362.3	0.0002
S_3	3.64	340.3	0.2686
exp[17c]		370[a]	
		keto-*s-trans*(−1)	
S_1	2.54	487.7 (518.5)	0.6445
S_2	2.75	450.3	0.0000
S_3	3.44	360.0	0.2562
exp[17c]		415[b]	
		keto-*s-cis*(−1)	
S_1	2.59	478.2	0.7135
S_2	2.78	446.3	0.0000
S_3	3.37	367.5	0.0000

[a] aqueous solution at pH=1. [b] aqueous solution at pH=10.

alternation, in the neutral form than in the anions. The C2−C2′ bond length in keto-s-trans (−1) is rather short (1.412 Å) indicative of strong conjugation in the −N=C−C=N−C=O linkage of the two rings. Another possible keto-structure, the keto-s-cis(−1) conformer, is only 5.3 kcal/mol higher in energy than the keto-s-trans(−1) and has similar geometrical parameters. Some of the earlier modeling studies[19] of the active site of luciferase plus substrate assumed a cis-geometry for the luciferin substrate.

The results from the TDDFT and ZINDO approaches for the singlet excited states of these forms of oxyluciferin are presented in Table 2. For all the keto-forms, the S_2 excitation is forbidden whereas the S_1 state is electric dipole allowed and corresponds to a HOMO to LUMO excitation. The KS frontier orbitals for the keto-forms are plotted in Figure 6. Changes in the absorption maxima, λ_{max}, from the neutral to the anionic keto-forms mirror structural trends which are similar to those observed in the LH_2 and LH_2 (−1) case. For the neutral keto-s-trans molecule, a large HOMO−LUMO gap of 3.63 eV is predicted from the KS eigenvalues. This HOMO−LUMO transition corresponds to a −N=C−C−N$^{\bullet}$ to −N$^{\bullet}$−C=C−N= rearrangement within the chromophore. As a result, the maximum of absorption is at 373.6 nm, close to that of neutral LH_2 where the bonding resembles the second valence bond structure. This result is in excellent agreement with the absorption maximum at 370 nm obtained for $OxyLH_2$ in water solution at pH = 1.[17c] On proceeding to keto-s-trans (−1), the HOMO changes dramatically and becomes similar to the LUMO as seen in Figure 6, with C2−C2′ essentially a double bond. The HOMO−LUMO gap calculated from the KS eigenvalues decreases to 2.42 eV and the absorption maximum is at 487.7 nm with the B3LYP TDDFT method. The absorption maximum at 415 nm observed for $OxyLH_2$ in water solution at pH = 10 [17c] lies between the absorption maxima of the limiting keto-s-trans and keto-s-trans (−1) structures. The keto-s-cis (−1) structure has very similar properties to the keto-s-trans(−1) conformer, with an insignificant blue shift in λ_{max}.

Enol-Forms of Oxyluciferin. The enolate- and enol-forms of $OxyLH_2$ could be formed easily from keto-$OxyLH_2$ in the S_1 excited state in the presence of base or acid and act in vivo as light emitters along with the keto-forms. Selected geometrical

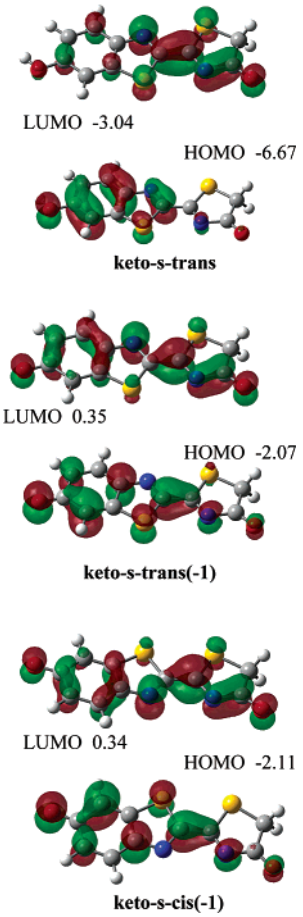

Figure 6. Kohn−Sham frontier orbitals for the keto-s-trans, keto-s-trans-(−1), and keto-s-cis(−1) structures of $OxyLH_2$ predicted with the B3LYP/6-31+G* method. The orbital energies are in eV.

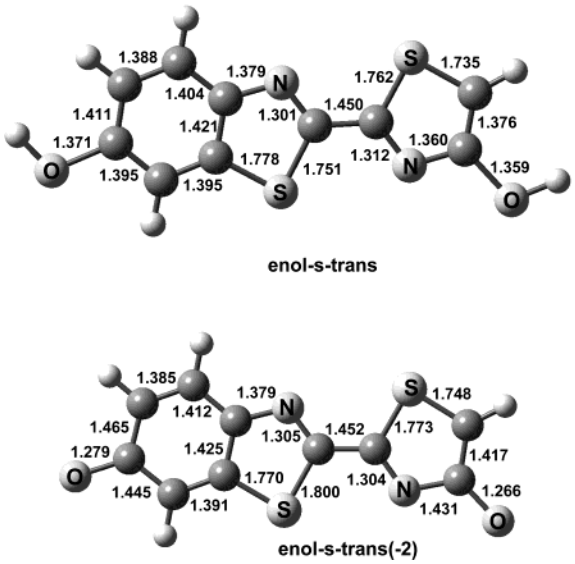

Figure 7. Selected geometrical parameters (in Å) for the enol-s-trans and enol-s-trans(−2) structures of $OxyLH_2$ with the B3LYP/6-31+G* method.

parameters of the four possible enol forms: neutral, enol-s-trans and dianion, enol-s-trans(−2), and of two anions, the enol-s-trans(−1) and enol-s-trans(−1)′, are shown in Figures 7 and 8. These systems represent limiting structures of the R_1...H...O(enol-$OxyLH_2$)O...H...R_2 complex. All structures have a slightly pyramidal C2′ atom. The neutral enol-s-trans and the

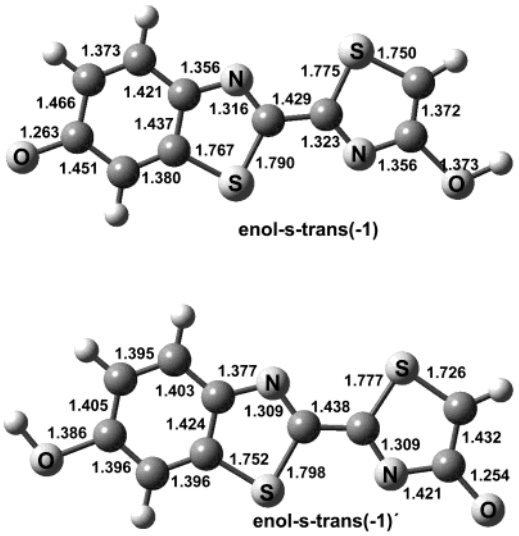

Figure 8. Selected geometrical parameters (in Å) for the enol-s-trans(−1) and enol-s-trans(−1)′ structures of $OxyLH_2$ with the B3LYP/6-31+G* method.

Table 3. Vertical Excitation Energies, ΔE, in eV, Excitation Wavelengths, λ, in nm (values in parentheses are from ZINDO), and Oscillator Strengths, *f*, Predicted for the First Three Singlet Excited States of and Enol-*s-trans*, Enol-*s-trans*(−1), Enol-*s-trans*(−2), and Enol-*s-trans*(−1)′ Forms of Oxyluciferin in the Gas Phase with TDDFT Using the B3LYP Functional and the 6-31+G* Basis Set

state	ΔE	λ	f
	enol-*s-trans*		
S_1	3.40	365.0 (371.9)	0.5519
S_2	3.85	322.1	0.0297
S_3	4.21	294.8	0.0162
	enol-*s-trans*(−1)		
S_1	2.48	499.9 (534.0)	0.6217
S_2	2.54	486.6	0.0021
S_3	2.88	430.3	0.0000
	enol-*s-trans*(−2)		
S_1	2.36	524.3 (516.0)	0.3003
S_2	2.63	472.0	0.0010
S_3	2.80	442.6	0.0001
	enol-*s-trans*(−1)′		
S_1	2.06	603.3 (595.4)	0.2304
S_2	2.24	553.6	0.0003
S_3	2.42	511.9	0.0044

anion, enol-s-trans (−1), are less stable by 8.5 and 19.9 kcal/mol than the corresponding keto-tautomers. Similar to the keto-forms, the −N═C−C═N- fragment with an essentially single C2−C2′ bond becomes more delocalized on proceeding from the neutral to the anionic form. The central C−C bond shortens and the C═N bonds lengthen. The dianion, enol-s-trans (−2), in contrast, has a localized −N═C−C═N- bonding arrangement, similar to the neutral enol-s-trans species. The C−C distance in the dianion is greater and the C═N bond length less than in the neutral compound.

Vertical excitation energies are given in Table 3 and the KS frontier orbitals are plotted in Figure 9 for the enol forms of oxyluciferin. The absorption spectrum of the neutral enol-s-trans structure is shifted to the blue, from 373.6 to 331.5 nm for $S_0 \rightarrow S_1$, compared to the keto-s-trans structure. In contrast, both the B3LYP TDDFT and ZINDO methods predict a small red shift for the absorption from enol-s-trans(−1) anion and a very large red shift for the enol-s-trans(−1)′ anion as compared

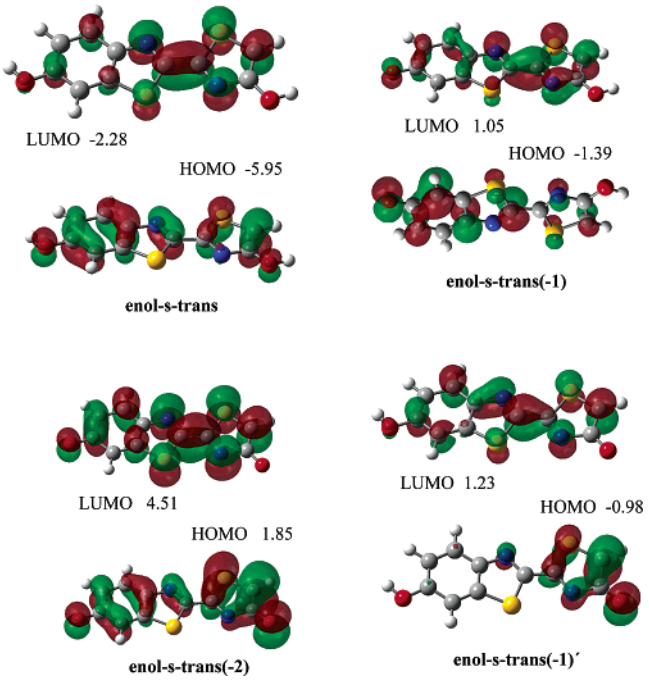

Figure 9. Kohn−Sham frontier orbitals for the enol-s-trans, enol-s-trans(−2), enol-s-trans(−1), and enol-s-trans(−1)′ structures of $OxyLH_2$ predicted with the B3LYP/6-31+G* method. The orbital energies are in eV.

to the keto-s-trans(−1). The enol-s-trans (−1)′ anion which has a fully protonated benzothiazolyl fragment and a completely deprotonated thiazol fragment would not emit visible light as its emission should be to the red of its predicted absorption maximum of 603.3 nm. Note that in vivo in the luciferase active site the benzothiazolyl hydoxyl group is almost certainly deprotonated. The data on the enol-s-trans (−1)′ anion is included here for completeness.

For the enol-s-trans (−2) dianion, B3LYP yields positive KS orbital energies for the LUMO and even for the HOMO (Figure 9). Under such circumstances, the predicted excitations from TDDFT must be viewed with some caution [25]. B3LYP TDDFT shifts the absorption maximum for the enol-s-trans (−2) to the red compared to the enol-s-trans (−1), whereas ZINDO reverses this ordering. The result from ZINDO is explicable since the LUMO of the enol-s-trans (−2) has more localized character than the LUMO of the enol-s-trans (−1). The ZINDO results suggest that simultaneous deprotonation of the two OH-group of the enol-form of $OxyLH_2$ may cause a smaller red shift than deprotonation of the benzothiazolyl fragment only.

Conclusions

The energetics of the reaction mechanisms predicted with the B3LYP/6-31G* method are supportive of the CIEEL theory. The spin-flip of triplet dioxygen to a singlet electronic state can proceed via an energetically feasible diradical mechanism in the presence of protonated His residue [30b,c]. The further formation of a dioxetanone intermediate in the $HisH^+...O_2^{-\bullet}...^{+\bullet}LH_2$ complex proceeds spontaneously as the AMP group found in nature is displaced. The ring opening and decarboxylation of dioxetanone proceed as a one-step reaction via a singlet diradical transition structure, with a barrier of 18.1 kcal/mol and reaction exothermicity to ground-state products of 90.8 kcal/mol. Excitation from the ground S_0 electronic state to the S_1 excited state requires ca. 80 and 60 kcal/mol for the neutral

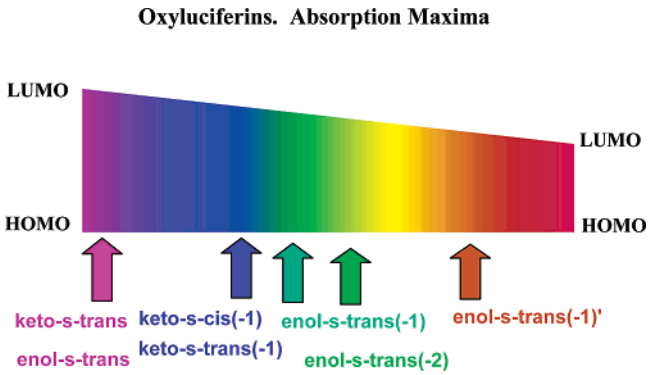

Figure 10. Theoretically predicted absorption maxima for the neutral and anionic forms of the keto- and enol-structures of $OxyLH_2$.

and anionic forms of $OxyLH_2$, respectively according to the TDDFT predictions.

Qualitatively, the $OxyLH_2$ structures may be divided into two groups on the basis of the HOMO−LUMO gaps and the absorption maxima, λ_{max}, as shown in Figure 10. The first group involves the neutral species, keto-s-trans, and enol-s-trans. The KS HOMO−LUMO gaps are large (ca. 3.6 eV) and the λ_{max} of absorption are in the range of 365 to 374 nm. The second group consists of the anions, keto-s-trans (−1), keto-s-cis (−1), enol-s-trans (−1), and enol-s-trans(−2). In this group, the HOMO−LUMO gaps are significantly smaller (ca. 2.4 eV) and the λ_{max} of absorption are in the range of 475 to 520 nm. An exception is the enol-s-trans (−1)′ anion which absorbs in the red and, therefore, should not emit in the visible. These neutral and anionic forms of $OxyLH_2$ represent the limiting cases of the $R_1...H...O$(keto-$OxyLH_2$) and $R_1...H...O$(enol-$OxyLH_2$)$O...H...R_2$ complexes where R_1 is a residue inside the luciferase pocket and R_2 is a residue or solvent molecule outside of the pocket (Recall Scheme 2.). The λ_{max} values vary depending on the polarization of the H−O bonds by R_1 and R_2. For keto-$OxyLH_2$, the R_1−H−O interaction inside the pocket is crucial. The smaller the H−O polarization, the greater the blue shift of the absorption. The enol-forms of $OxyLH_2$ manifest a more complicated dependence on polarization. For enol-s-trans (−1), the polarization of the H−O bond of the benzothiazolyl fragment by R_1 results in a red shift, similar to the keto-forms. The polarization of both H−O bonds by R_1 and R_2 causes a red-shift comparable to that caused by the polarization of the H−O bond of the benzothiazolyl fragment by R_1 only. For the enol-s-trans (−1)′ form, without a polarized H−O bond in the benzothiazolyl fragment (the least likely case), the polarization of the O−H bond of the thiazole fragment causes a large red shift, with absorption in the red resulting. Naturally, the polarization of these H−O bonds depends on the basicity of the R_1 and R_2 residues which can be changed through a hydrogen-bonding network by varying certain even remote residues.

Note that we have for the most part computed and discussed absorption spectra with the exception of the CIS results on emission in Figure 4. For all species, the emission must lie to the red of our predicted absorption maxima. The CIS results shown in Figure 4 do indicate that the shift in emission relative to absorption is 0.1 to 0.2 eV to lower energy.

The involvement of the twisted structures in bioluminescence appears less likely when the B3LYP DFT structures and the KS frontier orbitals are considered. The predicted C2−C2′ bond lengths reflect the conjugation across this bond which makes

internal rotation more difficult than predicted by the semiempirical AM1 model. The ab initio CIS model provides more direct evidence indicating that the essentially planar enol- and keto-forms of $OxyLH_2$ are both minima on the S_1 potential energy surface. The twisted excited-state ketone is not a minimum as presented in earlier semiempirical work.[16] The earlier result on the twisted keto-form of the excited state was verified with the AM1 method in MOPAC2002 [28a] but is a result of the known tendency of MNDO based models such as MNDO, AM1 and PM3 not to describe conjugated single bonds.[33,34]

The present predictions with TDDFT support the hypothesis that the color of bioluminescence depends on the polarization of the $OxyLH_2$ (namely, its H−O termini) in the microenvironment of the enzyme-$OxyLH_2$ complex. In general, a range of colors in the bioluminescence could be obtained with any of the forms of $OxyLH_2$ by this mechanism. The most likely light emitter is keto-s-trans (−1) but the enol-s-trans (−1) and keto-s-cis (−1) structures may also be involved. The mix of keto- and enol forms or of cis- and trans-forms is plausible but not necessary to explain the multicolor of the bioluminescence. The change in the strength of the interactions of R_1 and R_2 with H−O groups of $OxyLH_2$ can shift the emission of either the keto- or enol-forms providing a range of color. This conclusion that a mix of keto and enol oxyluciferin is not mandatory is in agreement with the recently reported experimental study by Branchini et al. [15] where multicolor luminescence was obtained from 5, 5-dimethyloxyluciferin which can exist only in the keto-form.

Acknowledgment. Financial support of this research by the Natural Sciences and Engineering Research Council of Canada (NSERC) is gratefully acknowledged.

Supporting Information Available: Total energies and Cartesian coordinates of all the reported structures are provided as Supporting Information. This material is available free of charge via the Internet at http://pubs.acs.org.

JA021255A